

# Towards the Quantum Internet: entanglement rate analysis of high-efficiency electro-optic transducer

Laura d’Avossa\*, Marcello Caleffi\*, Changqing Wang<sup>†</sup>, Jessica Illiano\*, Silvia Zorzetti<sup>†</sup>, Angela Sara Cacciapuoti\*

\* [www.QuantumInternet.it](http://www.QuantumInternet.it) research group, Department of Electrical Engineering and Information Technologies

<sup>\*</sup>Department of Electrical Engineering and Information Technology (DIETI)

<sup>†</sup>Fermi National Accelerator Laboratory, Batavia, IL, USA, 60510.

[lauradavossa@gmail.com](mailto:lauradavossa@gmail.com), [marcello.caleffi@unina.it](mailto:marcello.caleffi@unina.it), [cqwang@fnal.gov](mailto:cqwang@fnal.gov)

[jessica.illiano@unina.it](mailto:jessica.illiano@unina.it), [zorzetti@fnal.gov](mailto:zorzetti@fnal.gov), [angelasara.cacciapuoti@unina.it](mailto:angelasara.cacciapuoti@unina.it)

**Abstract**—Coherent microwave-optical photon conversion is a key enabling technology for the Quantum Internet, since it allows entanglement distribution among superconducting-based network nodes. A high-efficiency electro-optic transducer based on three-dimensional superconducting radio-frequency (SRF) technology has recently been proposed at Fermilab. In this paper, we evaluate the impact of Fermilab’s transduction hardware on the entanglement generation probability and the entanglement rate, which are two critical metrics from a communication engineering perspective. Furthermore, we provide some guidelines to increase the direct entanglement rate, i.e., the rate before any entanglement purification process. Our analysis shows that, through high-efficiency transduction, it is possible to reduce the network overhead. This preliminary work paves the way toward distantly interconnected superconducting quantum processors.

**Index Terms**—Quantum Internet, Transduction, Qubit, Coherence, Quantum networks, Entanglement, electro-optic transduction, EQT

## I. INTRODUCTION

The Quantum Internet is envisioned to be disruptive by enabling applications with no counterpart in the classical world [1]–[5], such as quantum distributed computing [6] and secure communications. The Quantum Internet [7] is a global quantum network that interconnects heterogeneous quantum networks. These interconnections rely on the capability of transferring quantum information, generating and distributing entanglement among the network nodes [2].

There is a wide consensus in the field to use optical photons, i.e., *flying quantum bits* (qubits), as entanglement carriers [7]. Whereas *matter qubits* represent the qubits needed for processing and storing the information within the quantum

The work of M. Caleffi was partially supported by the European Union under the Italian National Recovery and Resilience Plan (NRRP) of NextGenerationEU, partnership on “Telecommunications of the Future” (PE00000001 - program “RESTART” - E63C22002040007). Angela Sara Cacciapuoti acknowledges PNRR MUR NQSTI-PE000000023. Laura d’Avossa, Changqing Wang and Silvia Zorzetti acknowledge Fermi Research Alliance, LLC under Contract No. DE-AC02-07CH11359 with the U.S. Department of Energy, Office of Science, Office of High Energy Physics. L.d., C.W. and S.Z. also acknowledge the Fermilab’s Laboratory Directed Research and Development (LDRD) program and the U.S. Department of Energy, Office of Science, National Quantum Information Science Research Centers, Superconducting Quantum Materials and Systems Center (SQMS) under contract number DE-AC02-07CH11359.

nodes. In Fig. 1, we illustrate the role of transducers in converting matter-flying qubits.

Here, we focus on superconducting qubits as the most promising platform to encode fast gates and scale up quantum systems. High-efficiency quantum transducers are needed to coherently convert superconducting matter qubits to flying qubits. One way to realize such hybrid devices is by coupling electro-optic optical resonators with superconducting radio-frequency (SRF) cavities [8], [9]. Such electro-optic transducers use the Pockels effect to directly convert optical and microwave signals. Other transduction schemes may involve intermediate steps exploiting mediator modes that do not fall under either the microwave or optical spectra. They could be of a different nature, such as acoustic or mechanical, depending on the specific application and requirements for the system. A direct conversion is instead realized through electro-optic transducers, avoiding intermediate excitation that would increase the added noise of the system [10], [11].

In this paper, we first address the challenges arising from the design of the matter-flying transducer. We analyze two electro-optic transduction schemes: Direct Quantum Transduction (DQT) and Entanglement-based Quantum Transduction (EQT). We find an advantage in the EQT to generate and distribute entanglement, bypassing some of the demanding hardware requirements in the DQT [12]. Furthermore, EQT with generation of M-M entanglement avoids the direct transduction of the quantum information carrier with a subsequent reduction of the noise impact.

Then, we consider a high-efficiency electro-optic transduction technology based on three-dimensional SRF cavities, which is under development at Fermilab [8]. We perform a parametric analysis to evaluate entanglement generation probability and entanglement rate, critical metrics in quantum networks. Additionally, we provide some guidelines to increase the direct entanglement rate, i.e., the rate before any entanglement purification process. This is crucial, since purification increases the network overhead.

This preliminary work paves the way toward distantly interconnected superconducting quantum processors through high-efficiency transduction.

The paper is organized as follows. In Sec.II we pro-

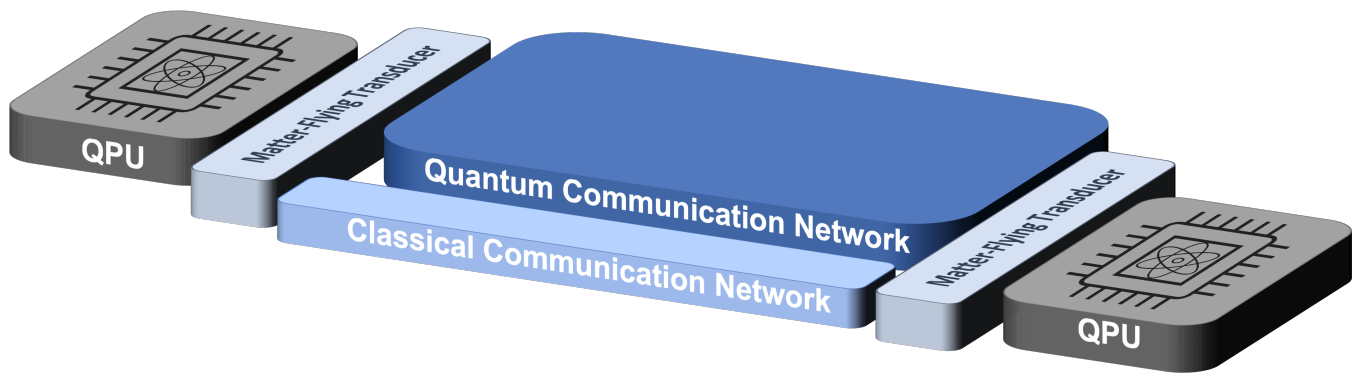


Fig. 1: Matter-flying transducer for remote quantum processing units (QPUs) interconnection. The matter-flying transducer is responsible for the bi-directional transduction between matter qubits and flying qubits.

vide an overview of matter-flying qubits and transduction schemes. In Sec. III, we further detail two different transduction schemes: DQT and EQT. Specifically, we highlight that the *entanglement-based quantum transduction* enables entanglement generation and distribution. In Sec. IV, we focus on heralded entanglement of microwave photons generation and distribution. In Sec. V we introduce an high efficiency - low loss transducer under development at Fermilab. Finally, to better understand the performance of such a transducer for quantum communications, we analyze two critical metrics in Sec. VI: entanglement generation probability and entanglement rate. This analysis is crucial to understand the key parameters affecting the performance of the matter-flying transducer in the light of the entanglement generation and distribution functionality for quantum networks.

## II. MATTER-FLYING QUBIT CONVERSION

### A. Matter-flying Transducer

Physical qubits, i.e. matter qubits, can be realized using several technologies, such as superconducting, ion traps-based, and photonic.

Ion traps are commonly recognized as efficient *quantum memories*, i.e., qubits dedicated to store quantum information, due to their notably long coherence time and their low interaction with the environment. Nevertheless, the low coupling with the environment, as well as the complex equipment required for the single ion addressing<sup>1</sup>, poses challenges in quantum computation based on ion qubits. Conversely, the superconducting technology stands out as the most promising platform for matter qubits with fast gates and high-scalability. However, superconducting qubits must be cooled down to milli-Kelvin temperatures and shielded in dilution refrigerators to avoid detrimental thermal noise, limiting the development of large-scale quantum networks, i.e., the interconnection of remote quantum processing units (QPUs). On the other hand, optical photons are immune to thermal noise at room

<sup>1</sup>Single ion addressing – the ability to act on a single ion without affecting the neighbouring ions. This operation is equivalent to performing a single-qubit gate and requires high precision lasers and complex control systems.

temperature and can be transmitted over long distances through optical fiber channels with extrimely low losses. As result, optical photons are usually referred to as flying qubits, which support the heralded generation and distribution [13], [14] of entangled states [15]. To realize a matter-flying qubit interface, superconducting and photonic technologies are combined into hybrid devices, i.e. *matter-flying* transducer.

One of the main challenges arising from the development of the matter-flying transducer concerns the frequency conversion between microwave and optical photons. Indeed, the conversion from matter qubits to flying qubits (and vice-versa) requires to mediate the huge energy gap between microwave frequencies (superconducting qubits) and optical frequencies (flying qubits), above five order of magnitude [16], [17]. Here, we identify the *electro-optic* transduction as a direct way to convert microwave to optical frequencies (up-conversion) and vice-versa (down-conversion).

### B. Electro-optic transduction

Electro-optic transduction is based on the Pockels effect and provides direct microwave-optical conversion, without intermediate mechanical resonators or local oscillators [9], which would increase the added noise in the frequency conversion. These hybrid devices comprise optical resonators coupled to microwave resonators. A laser pump mediates the interaction between the microwave and optical fields. The input classical laser pump can either be red or blue detuned. In *red-detuning*, the pump can trigger an up-conversion. In *blue-detuning*, it can trigger a down-conversion<sup>2</sup>. In both cases, the resulting phase modulation creates side-bands symmetrically placed around the optical pump frequency, that can be described by Sum Frequency Generation (SFG) and Difference Frequency Generation (DFG), respectively. They are also labelled as anti-Stokes and Stokes process [18].

<sup>2</sup>Colors red and blue are used to indicate two different optical pumping sidebands that are conventionally used in literature to distinguish pump lasers with different frequencies. Remarkably, they do not refer to red and blue frequencies in the optical spectrum.

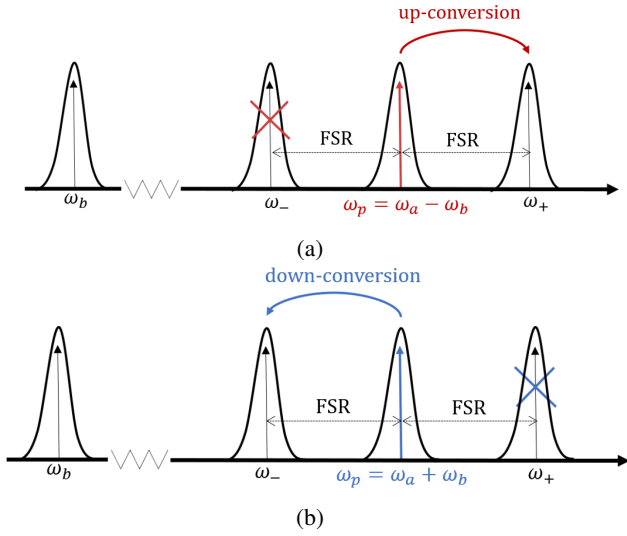


Fig. 2: Frequency spectrum for the output signal with red-detuned input pump power (a) and blue-detuned input pump power (b).

Let  $a$ ,  $a_1$ ,  $a_2$ ,  $b$  be the annihilation operators for the center optical mode, Stokes mode, anti-Stokes mode and microwave mode, and  $\omega_p$ ,  $\omega_-$ ,  $\omega_+$ ,  $\omega_b$  their respective frequencies. The Hamiltonian describing the three-wave mixing process is [19], [20]:

$$H = \hbar\omega_p a a^\dagger + \hbar\omega_- a_1 a_1^\dagger + \hbar\omega_+ a_2 a_2^\dagger + \hbar\omega_b b b^\dagger + \hbar g_0 (b + b^\dagger)(a + a_1 + a_2)^\dagger (a + a_1 + a_2) \quad (1)$$

where  $g_0$  denotes the nonlinear coupling rate [21]. In red-detuning, the frequency of the input pump is chosen as  $\omega_p = \omega_a - \omega_b$ . In this case, anti-Stokes and Stokes sidebands become respectively  $\omega_+ = (\omega_a - \omega_b) + \omega_b = \omega_a$  and  $\omega_- = (\omega_a - \omega_b) - \omega_b = \omega_a - 2\omega_b$ . However, if the free-spectral range ( $FSR$ ) of the optical cavity is equal to  $\omega_b$ , the red-detuned pump also leads to efficient down-conversion because of the presence of the resonant Stokes side-band. This undesired down-conversion can be suppressed either through off-resonance pumping and a detuning of  $\omega_b$  from the optical  $FSR$ , or by leveraging a center pump mode with a different polarization than the anti-Stokes mode [22]. Therefore, neglecting the Stokes mode ( $a_1$ ), the overall Hamiltonian of the system can be expressed as follows:

$$H = \hbar\omega_p a a^\dagger + \hbar\omega_+ a_2 a_2^\dagger + \hbar\omega_b b b^\dagger - g_0 \hbar (b + b^\dagger)(a + a_2)^\dagger (a + a_2) \quad (2)$$

Alternatively, we can realize a parametric down conversion. In this case the blue-detuned pump is excited at:  $\omega_p = \omega_a + \omega_b$ . We obtain  $\omega_+ = (\omega_a + \omega_b) + \omega_b = \omega_a + 2\omega_b$  and  $\omega_- = (\omega_a + \omega_b) - \omega_b = \omega_a$ . As for the red-detuned pump, the parametric up conversion could lead to the presence of the

resonant anti-Stokes side-band has to be suppressed. As result, the Hamiltonian of the system is:

$$H = \hbar\omega_p a a^\dagger + \hbar\omega_- a_1 a_1^\dagger + \hbar\omega_b b b^\dagger - g_0 \hbar (b + b^\dagger)(a + a_1)^\dagger (a + a_1) \quad (3)$$

where  $a_2$  is neglected. The frequency spectrum of the up/down-conversion is displayed in Figure 2 for the two different pumps and the corresponding Stokes and anti-Stokes side-bands generated.

### III. TRANSDUCTION SCHEMES

As discussed in the previous section, bidirectional microwave-optical transduction represents a pivotal building block for quantum networks.

We distinguish two main transduction schemes, namely [23]:

- Direct Quantum Transduction (DQT),
- Entanglement-based Quantum Transduction (EQT).

In order to obtain a point-to-point communication scheme exploiting, i.e., DQT, two transducers are required at i) the transmitter end for microwave-to-optical (M-O) conversion, and at ii) the receiver end for optical-to-microwave (O-M) conversion. The transducer at the transmitter converts the quantum state of a matter qubit into a photon, i.e., it maps the state encoded through the matter qubit into a flying qubit. The transducer at the receiver realizes the conversion in the opposite direction, i.e., O-M conversion and maps the state of the flying qubit into a matter qubit. It is noted that the DQT approach is highly demanding, as it requires both high coupling efficiency and small added noise [24] for both the M-O and O-M conversions [25]. If high pump power is applied to the optical system to realize the conversion, it leads to heating and thermal quasiparticles poisoning. Thus, a main technical challenge lies in finding the trade-off between the thermal noise and conversion efficiency [8], [24].

Here, we are considering EQT as an alternate scheme for entanglement generation and distribution. The interaction between microwave and optical light enables an important functionality for the network interface. Specifically, EQT allows to entangle microwave photons and optical photons, i.e., it generates entanglement between matter qubits and flying qubits [26]. This is a crucial result since entanglement represents a main resource for the Quantum Internet and quantum networks functionalities [15]. EQT first generates microwave-optical (M-O) entanglement [23], then it fulfill the state conversion through a beam-splitter, leveraging either M-O and M-M entanglement, according to the physical system. EQT first generates photons entanglement with parametric up- or down-conversion, then completes the state conversion through quantum teleportation. In the M-O case the quantum state to be distributed (denoted with  $|\psi\rangle$  by assuming a pure state) is stored within a superconducting qubit interconnected with the microwave resonator. A blue-detuned pump is applied to the cavity generating an entangled pair of optical and microwave photons. The microwave generated photon of the entangled

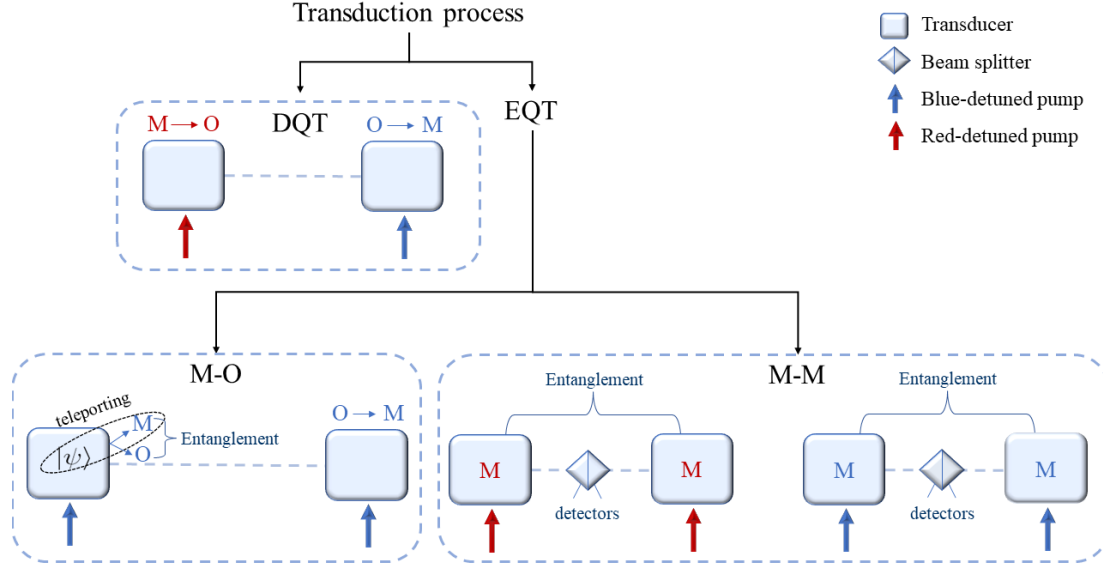


Fig. 3: Schematic depiction of three different schemes of transduction analyzed. Transducers are depicted with light blue squarrows. Blue- and red-detuned pump are depicted with narrows with the correspondent color.

pair and the superconducting qubit are processed as in a BSM interaction (thus, implementing a teleportation protocol). As a result, the state  $|\psi\rangle$  is now mapped on the optical photon that can reach the remote processor. After photon detection, the generated optical entangled photons reach the receiver through an optical fiber. Then, it is transduced back and elaborated by the destination system.

Both DQT and EQT with M-O entangled photons realize the connection between distant microwave quantum processors by converting the signal to the optical regime, and converting them back to microwaves. A schematic block diagram is available in Figure 3. Alternatively, the same goal can be accomplished through EQT with faithful M-M entanglement generation. The setup consists of two quantum transducers spatially separated. Both optical cavities are simultaneously excited with a laser pump and coupled to the respective optical fibers. The fibers transmit the generated optical photons to a beam splitter followed by two detectors without distinguishing among the different path information [25], [27]. The targeted entangled state to be generated is a Bell state between two distant microwave cavities, and it is identified by a single click of one detector [8], [25]. Figure 3 summarizes the different transduction schemes discussed so far.

#### IV. M-M ENTANGLEMENT BASED QUANTUM TRANSDUCTION

One of the main advantages of the EQT protocol with M-M entanglement is that microwave photons between remote superconducting QPUs are directly entangled. As the O-M reverse process is not required, EQT results in an enhanced fidelity of heralded entanglement. The photon generation in

one transducer under a continuous pump follows a Poissonian process [25] with photon generation rate given by:

$$r_0 = \frac{4g_0\langle n_p\rangle\gamma_{a,c}}{(\gamma_{a,c} + \gamma_{a,0})^2} \quad (4)$$

where  $\gamma_{a,c}$  and  $\gamma_{a,0}$  denote extrinsic and intrinsic loss rate of the optical modes (i.e., the pump and the optical mode in the cavity), respectively. While,  $\langle n_p\rangle$  denotes the average number of photons in the pump mode and depends on both input pump power ( $P_{in}$ ) and optical losses  $\gamma_{a,c}$  and  $\gamma_{a,0}$  as follows:

$$\langle n_p\rangle = \frac{4\gamma_{a,c}}{(\gamma_{a,c} + \gamma_{a,0})^2} \frac{P_{in}}{\hbar\omega_p} \quad (5)$$

Assuming a fixed duration time of the transduction process, i.e., the duration of each pump pulse ( $\Delta t$ ), the click rate of the detector is given by<sup>3</sup>:

$$r_c = 2r_0 e^{-r_0\Delta t} \frac{\Delta t}{\Delta t + t_r} \quad (6)$$

where  $t_r$  is the microwave reset time after each generation event and it is usually set equal to  $1\mu s$ . The factor two in (6) comes from the fact that each of the two nodes can produce a heralded photon [25].

As previously mentioned, in order to successfully herald the M-M entanglement, we need optical single photon clicks by the detector. This click-based entanglement swapping scheme is probabilistic, as discussed in Ref. [24]. With the EQT M-M transduction scheme, we may either operate with red- or blue-detuned pump.

<sup>3</sup>It is important to emphasize that in some previous works [8] and [25] ( $r_e$ ) refers to the *entanglement rate*. Instead, in this work,  $r_c$  refers to the possibility of a single click of the detector. We will define entanglement rate the product between  $r_c$  and the entanglement generation probability.

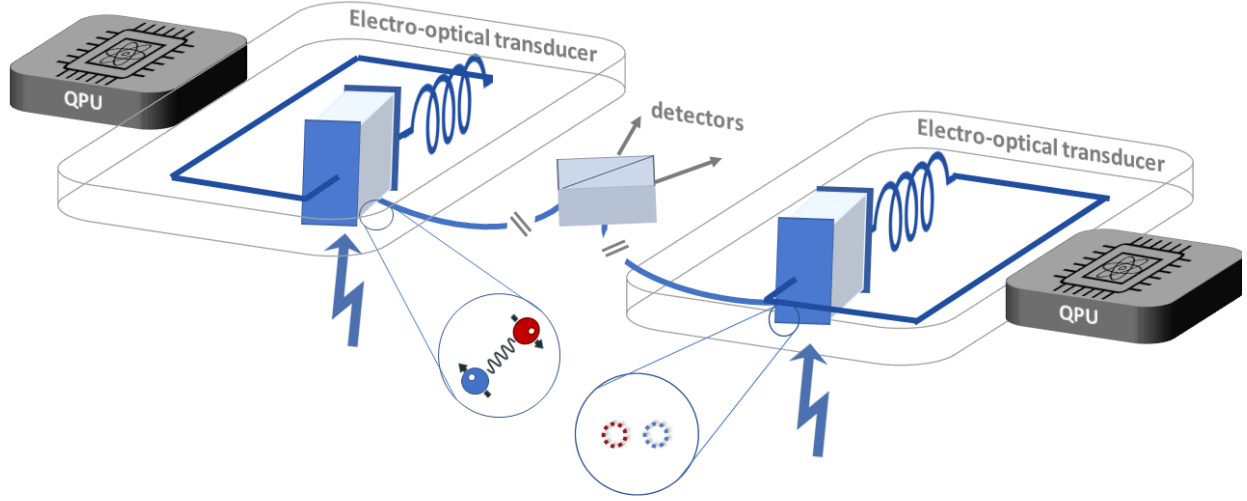


Fig. 4: M-M entanglement generation and distribution with blue-detuned pump. A pump optical photon can be converted into a microwave and an optical photon. The microwave photon generated in one transducer is indicated with blue, the optical photon generated is depicted with red. Differently, dotted circles represent the event *no entangled photons generated*.

First, we consider the blue-detuned pumping case. The probability that a single photon is generated in the microwave cavity is expressed as:

$$P_1 = r_0 \Delta t e^{-r_0 \Delta t}. \quad (7)$$

While the probability that no photon is generated is:

$$P_0 = e^{-r_0 \Delta t} \quad (8)$$

Figure 4 schematically show the microwave and optical photon generation, with probability  $P_{10}$  in blue-detuned pumping case.

In particular, to identify an entangled state, the detection of a single optical photon is required [8], [25]. However, it is possible that the down-conversion process simultaneously produce a microwave photon in each of the two resonators. This probability is given by:

$$P_{11} = P_1^2 \quad (9)$$

As a result, the detection is affected by uncertainty. Indeed, a detector click can also indicate the presence of two microwave photons in the cavities that, as consequence, are not entangled. This leads to the possibility that multiple photons may be produced within a single microwave cavity. The probability of observing more than one photon within a single microwave cavity is:

$$P_{m>1, n \leq 1} = P_{m \leq 1, n > 1} = (1 - P_0 - P_1)(P_0 + P_1) \quad (10)$$

The probability that more than one photon is generated in each cavity is given by:

$$P_{m>1, n > 1} = (1 - P_0 - P_1)^2 \quad (11)$$

The final state of the system is the superposition of two-photon *Fock states*. We denote a Fock state with  $|n_a n_b\rangle$ , where  $n_a$  and  $n_b$  represent the optical photon generated by the first and the second transducer respectively [25]. The final state of the system can be written as:

$$\begin{aligned} |\psi_f\rangle = & \sqrt{P_{00}} |00\rangle + \sqrt{P_{01}} |01\rangle + \sqrt{P_{10}} |10\rangle + \sqrt{P_{11}} |11\rangle \\ & + \sqrt{P_{m>1, n \leq 1}} |m > 1, n \leq 1\rangle + \sqrt{P_{m \leq 1, n > 1}} |m \leq 1, n > 1\rangle \\ & + \sqrt{P_{m>1, n > 1}} |m > 1, n > 1\rangle \end{aligned} \quad (12)$$

The *entanglement generation probability* is expressed as<sup>4</sup>:

$$P_{e,b} = \frac{P_{10} + P_{01}}{P_{10} + P_{01} + P_{11} + P_{m>1, n \leq 1} + P_{m \leq 1, n > 1} + P_{m>1, n > 1}} \quad (13)$$

where the subscript  $b$  refers to the blue-detuned pump. In (13) we do not consider  $P_{00}$ . Indeed, because no optical photons reach the beam-splitter, there is no click of the detectors indicating the entanglement generation. Thus, the probability

<sup>4</sup>It is important to emphasize that in some previous works [8] (13) refers to *fidelity*. Instead, in this work,  $P_{e,b}$  refers to the probability that with a blue input pumping a single click of the detector indicates the presence of entanglement between distant processors. Same considerations hold for  $P_{e,r}$  considering red input pumping.

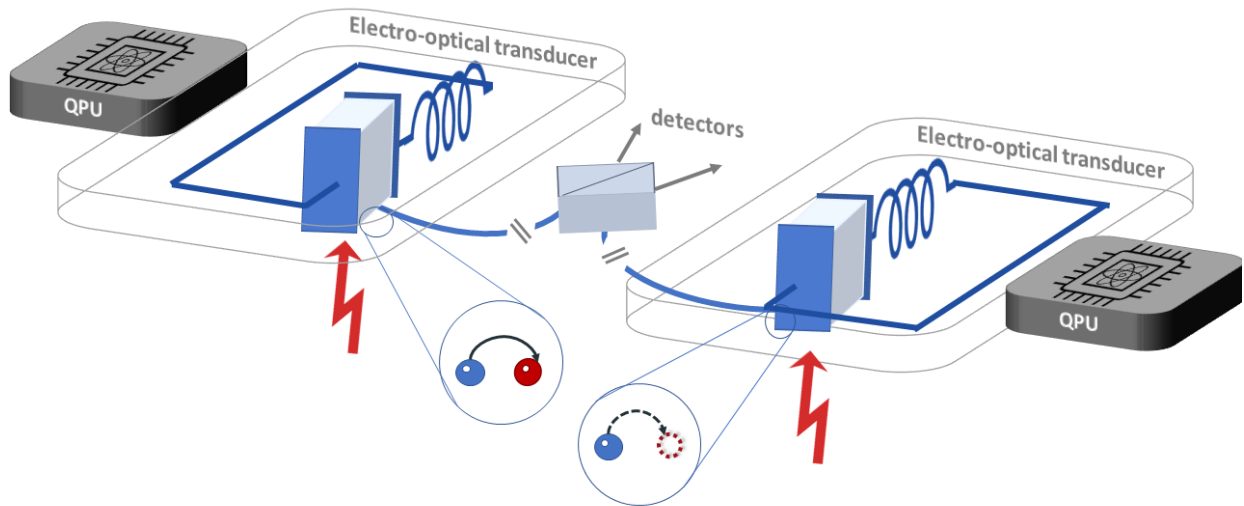


Fig. 5: M-M entanglement generation and distribution with red-detuned pump. Firstly, both microwave cavities are prepared with one photon state while leaving the optical cavity at the zero-photon state. A microwave photon can be converted to an optical photon (red circle).

that both transducers do not generate optical photons does not affect the entanglement generation probability. The entanglement generation probability of heralded entanglement is likely to be compromised for two reasons. On one hand, the down-conversion process can generate states that contain more than one photon. On the other hand, there is a low probability that the down-conversion process generates a photon in each of the two resonators simultaneously.

While the second source of reduction of entanglement generation probability is unavoidable ( $P_{11}$ ), the first one can be eliminated using a red-detuned pump instead of a blue-detuned pump [25]. To enable remote entanglement with red-sideband pumping, both microwave cavities are prepared with one microwave photon. The probability that this photon is converted into an optical photon is:

$$P_1 = 1 - e^{-r_0 \Delta t} \quad (14)$$

The probability that no optical photons are generated is:

$$P_0 = e^{-r_0 \Delta t} \quad (15)$$

In this case, the final state can be expressed as:

$$|\psi_f\rangle = \sqrt{P_{00}}|00\rangle + \sqrt{P_{01}}|01\rangle + \sqrt{P_{10}}|10\rangle + \sqrt{P_{11}}|11\rangle \quad (16)$$

With red-detuned pump, the the entanglement generation probability is only affected by  $P_{11} = P_1^2$ . In fact, the red-detuned pumping case adopts a direct transduction from the microwave photon to the optical one. As result, no new microwave photons are created. Thus, we enhance the fidelity of the heralded

Probability	Cavity 1		Cavity 2	
	Microwave	Optical	Microwave	Optical
$P_{00}$	$ 1\rangle$	$ 0\rangle$	$ 1\rangle$	$ 0\rangle$
$P_{01}$	$ 1\rangle$	$ 0\rangle$	$ 0\rangle$	$ 1\rangle$
$P_{10}$	$ 0\rangle$	$ 1\rangle$	$ 1\rangle$	$ 0\rangle$
$P_{11}$	$ 0\rangle$	$ 1\rangle$	$ 0\rangle$	$ 1\rangle$

TABLE I: Red-detuned pump microwave and optical photons generation events.

entanglement. Figure 5 schematically represents microwave to optical photon transition with probability  $P_{10}$  with red-detuned pump.

Table I shows possible cases of microwave and optical photon present in the transducer with red-detuned pump. Excluding terms indicating the generation of more than one microwave photon, Table I also holds for the blue-detuned pumping case. However, it is noted that, in the red-detuned pumping case the  $|0\rangle$  indicated in the microwave columns refers to a successful conversion of the microwave photon into an optical photon. Instead, in the blue-detuned pumping case, the  $|0\rangle$  indicated in the microwave columns refers to a failed generation of an entangled M-O pair. The entanglement generation probability is given by:

$$P_{e,r} = \frac{P_{10} + P_{01}}{P_{10} + P_{01} + P_{11}} \quad (17)$$

where the subscript  $r$  refers to the red-detuned pump adopted. As result, without the factors  $P_{m>1,n\leq 1}$ ,  $P_{m\leq 1,n>1}$ ,  $P_{m>1,n>1}$

the entanglement generation probability with red-detuned pump is improved. Furthermore, if  $P_{11} = 0$ , it reaches the maximum possible value, i.e.,  $P_{e,r} = 1$ . Following this approach, the quantum state of interest is never truly carried by the optical mode, as conversely done by both DQT and EQT with M-O entanglement generation. The optical photon is instead used only to entangle two microwave photons excited in each microwave cavity [25]. The detection of the optical photon is only necessary to herald the generation of the pair of microwave entangled photons in the two distant cavities.

### V. 3D ELECTRO-OPTIC TRANSDUCER

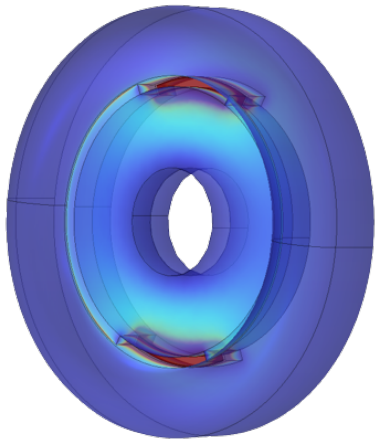


Fig. 6: Three-dimensional superconducting RF (SRF) cavity and electro-optic design for quantum transduction.

Different systems are being evaluated to realize efficient microwave-optical conversion at the quantum threshold, i.e. quantum transduction. As noted, electro-optic transduction provides a direct conversion. The limit in the current state-of-the-art electro-optic transducers is the need of high pump power that leads to high photon loss. Indeed, when the pump power applied to the optical resonator is high, the interaction between optical and microwave photons increases. However, the high optical pumping leads to overheating and is in conflict with the critical temperature required for superconducting qubits operation ( $< 120$  mK). Thus, a trade-off between thermal noise and transduction efficiency is needed. A novel hardware platform implemented at Fermilab and supported by Superconducting Quantum Materials and Systems (SQMS) Center [8] could greatly overcome this issue by increasing the microwave quality factor. In currently available electro-optic transducers, while the optical quality factor ( $Q_a$ ) can reach the order of  $10^7$ , the microwave quality factor ( $Q_b$ ) is bounded by lower values ( $< 10^3$ ). The proposed device consists of an lithium niobate (LN) whispering gallery mode (WGM) optical resonator enclosed by a 3D bulk niobium SRF cavity (Figure 6). In order to obtain a good microwave-optical interaction while maintaining a low input pump power, the quality factor of the system is increased by careful microwave

design and fields alignment. The microwave quality factor at cryogenic temperatures is mainly determined by the losses in the dielectric crystal but it also has a trade-off with the single-photon electro-optic coupling coefficient, which is determined by the overlap between microwave and optical fields. In the transduction system under evaluation at Fermilab the losses are mostly concentrated in the dielectric LN resonator, which defines the internal quality factor of the microwave cavity. Moreover, to obtain a good interaction between microwave and optical fields, the quality factor of the system is increased by careful microwave design and fields alignment. With this architecture, the system could reach a microwave quality factor of about  $10^5$ . Therefore, this hardware represents a critical interface that enables to: i) enable operations in current dilution refrigerators, ii) interconnect superconducting quantum processors, iii) share remote entanglement through optical fibers [8].

### VI. PERFORMANCE ANALYSIS

Our goal is to analyze the performance of Fermilab’s high-efficiency transducer in quantum network applications. We exploit M-M entanglement-based (EQT) transduction using the proposed hardware for maximizing the two key metrics affecting the system’s communications performances, which are the entanglement generation probability and the entanglement rate. We model the network using transduction parameters as in Ref. [8]. In particular, we use the input pump power  $P_{in}$  and the coupling strength, i.e., the ratio between extrinsic loss rate of the optical mode ( $\gamma_{a,c}$ ) normalized by the intrinsic optical loss rate denoted with ( $\gamma_{a,0}$ ). Both these factors act on the photon generation rate, expressed in (4), and consequently on the click rate, expressed in (6).

A high-index prism is placed close to the rim of the optical resonator to couple the optical pump into the WGM of the proposed system [28]. The coupling strength between the resonator and the prism is controlled by their spatial gap. The prism has a negligible effect on the microwave loss [29]. We derive the click rate as a function of the coupling strength and the input pump power. We vary the coupling strength in the range  $[1 - 10]$ , typical values of this parameter for the system in exam, and the input pump power in  $[100 \mu W - 1 mW]$ , i.e., the range of power values at which the transducer typically works. The duration time of the transduction process and the reset time are fixed, both equal to about  $1 \mu s$  (typical values for these parameters). Figure 7a shows the click rate  $r_c$  as a function of the coupling strength  $\frac{\gamma_{a,c}}{\gamma_{a,0}}$  (linear scale) and the pump input power  $P_{in}$  (logarithmic scale). The click rate increases with the input pump power and reaches a maximum ( $\sim 3.6 \times 10^5$  Hz) at  $P_{in} \simeq 1 mW$  and  $\frac{\gamma_{a,c}}{\gamma_{a,0}} \simeq 1.5$ . We then evaluate entanglement generation probability of the click rate to optimize the communication performance.

We also examine the entanglement generation probability of the click rate as a function of  $\frac{\gamma_{a,c}}{\gamma_{a,0}}$  and  $P_{in}$ . Due to previously mentioned performance optimization purposes, we adopt a red-detuned input pumping. Figure 7b shows the difference

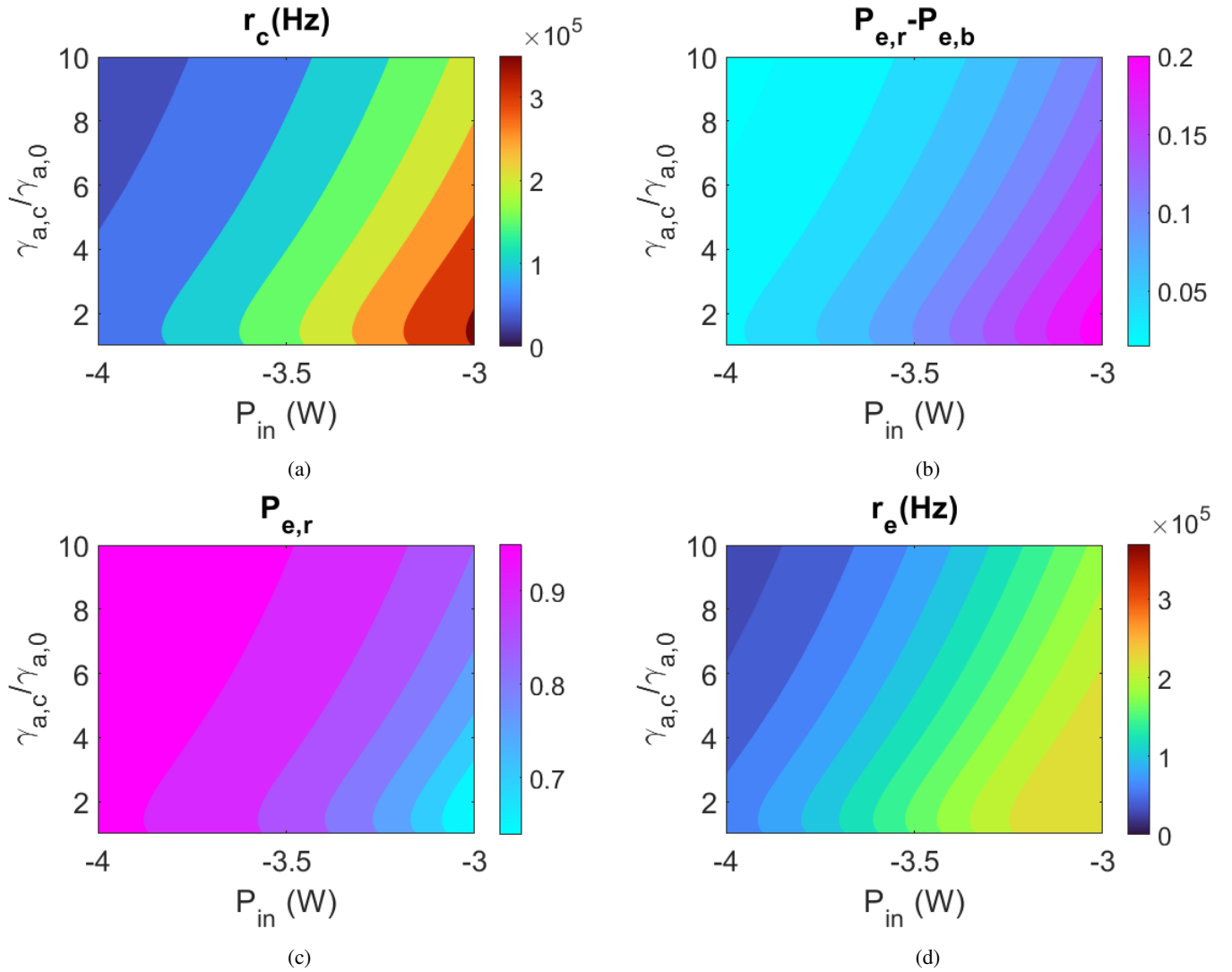


Fig. 7: Detector click rate  $r_c$  (a), difference between entanglement generation probability with red- and blue- detuning case  $P_{e,r} - P_{e,b}$  (b) entanglement generation probability in red-detuning case  $P_{e,r}$  (c) and entanglement rate  $r_e$  (d) as a function of the coupling strength  $\frac{\gamma_{a,c}}{\gamma_{a,0}}$  and input pump power  $P_{in}$ . It is important to emphasize that in some previous works [8]  $r_c$  expressed with (6) and  $P_{e,r}$  expressed with (13) are called *entanglement rate* and *fidelity*, respectively. However, in this case,  $r_e$  refers to the possibility of a single click of the detector and  $P_{e,r}$  refers to the probability that a single click of the detector indicates the presence of entanglement between distant processors.

between entanglement generation probability in case of red-detuned pumping  $P_{e,r}$  and entanglement generation probability in case of blue-detuned pumping  $P_{e,b}$ . It is clear that  $P_{e,r}$  is higher than  $P_{e,b}$  for every value of  $\frac{\gamma_{a,c}}{\gamma_{a,0}}$  and  $P_{in}$ . The difference reaches its minimum ( $\sim 0.1$ ) for  $P_{in} \sim 100 \mu W$ . We find that the red-detuned pumping scheme is a better fit for applications related to the quantum internet as it leads to higher entanglement generation probability. Figure 7c shows that, differently from  $r_c$ ,  $P_{e,r}$  increases with the decreasing of  $P_{in}$ . Moreover, it also increases with  $\frac{\gamma_{a,c}}{\gamma_{a,0}}$ . This means that the corresponding click rate represents the *direct entanglement rate* i.e., a click of the detector corresponds to the presence of

entanglement between processors and does not require further *purification*. To take into account the analysis results obtained (Figure 7a and Figure 7c) and therefore to meet the trade-off between click rate and entanglement generation probability, we estimate their product  $r_e = r_c \times P_{e,r}$  (Figure 7d), i.e. the entanglement rate. Comparing Figure 7a and Figure 7d, it is clear that for low values of  $P_{in}$ ,  $r_c$  and  $r_e$  assume similar values. However, by increasing  $P_{in}$  the entanglement rate decreases compared to the correspondent value of the click rate. For instance, while for  $P_{in} \simeq 1 mW$  and  $\frac{\gamma_{a,c}}{\gamma_{a,0}} \simeq 1.5$ ,  $r_c$  reaches its maximum ( $\sim 3.6 \times 10^5 Hz$ ),  $r_e$  reaches  $\simeq 2.2 \times 10^5 Hz$ . This is due to the value of the entanglement generation probability

that results less than 1. As expected, this analysis also supports network operations at lower input power pump. The maximum value of the entanglement rate ( $P_{e,r} \simeq 1$ )  $7 \times 10^4$  Hz is obtained at  $P_{in} \simeq 100 \mu W$  and  $\frac{\gamma_{a,c}}{\gamma_{a,0}} \simeq 1.5$ . A main finding of this work is that by decreasing the input power pump, the gap between  $r_c$  and  $r_e$  decreases. This is valid for fixed values of  $\Delta t$  and  $t_r$ . Moreover, this enhancement of the entanglement generation is possible without additional entanglement purification. Remarkably this also results in a reduction of the maximum value of entanglement generation.

## VII. CONCLUSIONS

The quantum transduction of microwave and optical fields is currently a very active area of research. Here, we discussed microwave-optical transduction in the light of network functionalities for the interconnection of remote superconducting-based quantum processing units. Specifically, we underlined that coherent microwave-optical conversion of single photons enables the exchange of quantum states between remotely connected QPUs. We discussed the role of quantum transduction for the network interface and recognized its pivotal capability to entangle microwave and optical photons. More into details, we conducted a performance analysis from a communication point of view by focusing on entanglement-based quantum transduction, and we discussed how the EQT scheme enables M-M entanglement generation with high fidelity. Among the latest transduction devices proposal, Fermilab proposes an electro-optic transducer capable of achieving high conversion efficiency maintaining low incoming pump power. We evaluated the Fermilab's system to realize the interconnection between remote superconducting quantum processors through heralded entanglement generation and distribution. In particular, we tuned the above hardware parameters through numerical simulations to achieve maximum click rate and entanglement generation probability with a low input power pump. We obtained an entanglement rate of  $\sim 7 \times 10^4$  Hz with a red-detuned input power pump of  $\sim 100 \mu W$  and a coupling strength of  $\sim 1.5$ . We find that the entanglement generation probability close to 1, i.e., the click rate corresponds to the entanglement rate ( $r_c = r_e$ ), and thus to the direct entanglement rate. This platform holds great potential for the near-future realization the Quantum Internet.

## REFERENCES

- [1] H. J. Kimble, "The quantum internet," *Nature*, vol. 453, no. 7198, pp. 1023–1030, 2008.
- [2] A. S. Cacciapuoti, M. Caleffi, F. Tafuri, F. S. Cataliotti, S. Gherardini, and G. Bianchi, "Quantum internet: Networking challenges in distributed quantum computing," *IEEE Network*, vol. 34, no. 1, pp. 137–143, 2020.
- [3] W. Dür, R. Lamprecht, and S. Heusler, "Towards a quantum internet," *European Journal of Physics*, vol. 38, no. 4, p. 043001, 2017.
- [4] S. Wehner, D. Elkouss, and R. Hanson, "Quantum Internet: a Vision for the Road Ahead," *Science*, vol. 362, no. 6412, 2018.
- [5] R. V. Meter, R. Satoh, N. Benchasatabuse, K. Teramoto, T. Matsuo, M. Hajdusek, T. Satoh, S. Nagayama, and S. Suzuki, "A quantum internet architecture," *2022 IEEE International Conference on Quantum Computing and Engineering (QCE)*, pp. 341–352, sep 2022.
- [6] M. Caleffi, M. Amoretti, D. Ferrari, D. Cuomo, J. Illiano, A. Manzalini, and A. S. Cacciapuoti, "Distributed quantum computing: a survey," *arXiv preprint arXiv:2212.10609*, 2022.

- [7] W. Kozłowski, S. Wehner, R. V. Meter, B. Rijsman, A. S. Cacciapuoti, M. Caleffi, and S. Nagayama, "Architectural Principles for a Quantum Internet," RFC 9340, Mar. 2023. [Online]. Available: <https://www.rfc-editor.org/info/rfc9340>
- [8] C. Wang and S. Zorzetti, "High-fidelity quantum transduction with long coherence time superconducting resonators," *Quantum 2.0 Conference and Exhibition*, p. QTu2A.7, 2022. [Online]. Available: <https://opg.optica.org/abstract.cfm?URI=QUANTUM-2022-QTu2A.7>
- [9] N. Lauk, N. Sinclair, S. Barzanjeh, J. Covey, M. Saffman, M. Spiropulu, and C. Simon, "Perspectives on quantum transduction," *Quantum Science and Technology*, vol. 5, 02 2020.
- [10] J. Wu, C. Cui, L. Fan, and Q. Zhuang, "Deterministic microwave-optical transduction based on quantum teleportation," *Phys. Rev. Appl.*, vol. 16, p. 064044, Dec 2021. [Online]. Available: <https://link.aps.org/doi/10.1103/PhysRevApplied.16.064044>
- [11] X. Han, W. Fu, C.-L. Zou, L. Jiang, and H. X. Tang, "Microwave-optical quantum frequency conversion," *Optica*, vol. 8, no. 8, pp. 1050–1064, Aug 2021. [Online]. Available: <https://opg.optica.org/optica/abstract.cfm?URI=optica-8-8-1050>
- [12] C. Zhong, Z. Wang, C. Zou, M. Zhang, X. Han, W. Fu, M. Xu, S. Shankar, M. H. Devoret, H. X. Tang, and L. Jiang, "Proposal for heralded generation and detection of entangled microwave-optical-photon pairs," *Phys. Rev. Lett.*, vol. 124, p. 010511, Jan 2020. [Online]. Available: <https://link.aps.org/doi/10.1103/PhysRevLett.124.010511>
- [13] S. Barz, G. Cronenberg, A. Zeilinger, and P. Walther, "Heralded generation of entangled photon pairs," *Nature photonics*, vol. 4, no. 8, pp. 553–556, 2010.
- [14] J. Hofmann, M. Krug, N. Ortegel, L. Gérard, M. Weber, W. Rosenfeld, and H. Weinfurter, "Heralded entanglement between widely separated atoms," *Science*, vol. 337, no. 6090, pp. 72–75, 2012.
- [15] J. Illiano, M. Caleffi, A. Manzalini, and A. S. Cacciapuoti, "Quantum internet protocol stack: A comprehensive survey," *Computer Networks*, p. 109092, 2022.
- [16] A. S. Cacciapuoti, M. Caleffi, F. Tafuri, F. S. Cataliotti, S. Gherardini, and G. Bianchi, "Quantum internet: Networking challenges in distributed quantum computing," *IEEE Network*, vol. 34, no. 1, pp. 137–143, 2020.
- [17] A. S. Cacciapuoti, M. Caleffi, R. Van Meter et al., "When entanglement meets classical communications: Quantum teleportation for the quantum internet," *IEEE Trans. on Communications*, vol. 68, no. 6, pp. 3808–3833, 2020, invited paper.
- [18] A. Rueda, F. Sedlmeir, M. C. Collodo, U. Vogl, B. Stiller, G. Schunk, D. V. Strekalov, C. Marquardt, J. M. Fink, O. Painter, G. Leuchs, and H. G. L. Schwefel, "Efficient microwave to optical photon conversion: an electro-optical realization," *Optica*, vol. 3, no. 6, pp. 597–604, Jun 2016. [Online]. Available: <https://opg.optica.org/optica/abstract.cfm?URI=optica-3-6-597>
- [19] V. S. Ilchenko, A. A. Savchenkov, A. B. Matsko, and L. Maleki, "Whispering-gallery-mode electro-optic modulator and photonic microwave receiver," *J. Opt. Soc. Am. B*, vol. 20, no. 2, pp. 333–342, Feb 2003. [Online]. Available: <https://opg.optica.org/josab/abstract.cfm?URI=josab-20-2-333>
- [20] A. B. Matsko, A. A. Savchenkov, V. S. Ilchenko, D. Seidel, and L. Maleki, "On fundamental quantum noises of whispering gallery mode electro-optic modulators," *Opt. Express*, vol. 15, no. 25, pp. 17401–17409, Dec 2007. [Online]. Available: <https://opg.optica.org/oe/abstract.cfm?URI=oe-15-25-17401>
- [21] M. Tsang, "Cavity quantum electro-optics," *Phys. Rev. A*, vol. 81, p. 063837, Jun 2010. [Online]. Available: <https://link.aps.org/doi/10.1103/PhysRevA.81.063837>
- [22] —, "Cavity quantum electro-optics. ii. input-output relations between traveling optical and microwave fields," *Phys. Rev. A*, vol. 84, p. 043845, Oct 2011. [Online]. Available: <https://link.aps.org/doi/10.1103/PhysRevA.84.043845>
- [23] C. Zhong, X. Han, H. X. Tang, and L. Jiang, "Entanglement of microwave-optical modes in a strongly coupled electro-optomechanical system," *Phys. Rev. A*, vol. 101, p. 032345, Mar 2020. [Online]. Available: <https://link.aps.org/doi/10.1103/PhysRevA.101.032345>
- [24] C. Zhong, X. Han, and L. Jiang, "Microwave and optical entanglement for quantum transduction with electro-optomechanics," *Phys. Rev. Appl.*, vol. 18, p. 054061, Nov 2022. [Online]. Available: <https://link.aps.org/doi/10.1103/PhysRevApplied.18.054061>
- [25] S. Krastanov, H. Raniwala, J. Holzgrafe, K. Jacobs, M. Lončar, M. J. Reagor, and D. R. Englund, "Optically heralded entanglement of superconducting systems in quantum networks," *Phys. Rev.*

- Lett., vol. 127, p. 040503, Jul 2021. [Online]. Available: <https://link.aps.org/doi/10.1103/PhysRevLett.127.040503>
- [26] R. Andrews, R. Peterson, T. Purdy, K. Cicak, R. Simmonds, C. Regal, and K. Lehnert, "Bidirectional and efficient conversion between microwave and optical light," *Nat. Phys.*, vol. 10, 03 2014.
- [27] R. Pakniat, M. H. Zandi, and M. K. Tavassoly, "On the entanglement swapping by using the beam splitter," *European Physical Journal Plus*, vol. 132, no. 1, p. 3, Jan. 2017.
- [28] M. L. Gorodetsky and V. S. Ilchenko, "Optical microsphere resonators: optimal coupling to high-q whispering-gallery modes," *J. Opt. Soc. Am. B*, vol. 16, no. 1, pp. 147–154, Jan 1999. [Online]. Available: <https://opg.optica.org/josab/abstract.cfm?URI=josab-16-1-147>
- [29] M. Cai, O. Painter, and K. J. Vahala, "Observation of critical coupling in a fiber taper to a silica-microsphere whispering-gallery mode system," *Phys. Rev. Lett.*, vol. 85, pp. 74–77, Jul 2000. [Online]. Available: <https://link.aps.org/doi/10.1103/PhysRevLett.85.74>